Turkish Journal of Science & Technology
18(1), 45-57, 2023

Research Paper
https://doi.org/10.55525/tjst.1170464

The Effects of Hydroxyapatite on the Corrosion Behaviour of AZ Series Mg Alloys

Yakup SAY[1*]

[1]Department of Machine and Metallic Technology, Munzur University, Tunceli, Turkey
[*1]yakupsay@gmail.com

(Geliş/Received: 03/09/2022; Kabul/Accepted: 29/10/2022)

Abstract: Metallic biomaterials are widely used in the orthopedic and dental applications owing to their advanced biocompatibility and sophisticated mechanical properties. Many studies are carried out to develop new alloys with high specific strength, high corrosion resistance and high biocompatibility as an alternative to present metallic biomaterials. Mg alloys are potential alloys as a biomaterial, especially because they have low density and high biocompatibility. However, especially the corrosion properties of Mg alloys need to be improved. In this study, the surfaces of AZ31, AZ61 and AZ91 alloys, which are promising as biomaterials, were coated with hydroxyapatite with high biocompatibility, and the effects of the bioceramics coatings on corrosion resistance were comprehensively investigated. Crack-free and porous surface morphologies were obtained in all bioceramic coatings and the presence of the coatings on the surfaces was supported by EDS analysis. As a result of the corrosion tests performed in SBF, it was determined that the AZ91 alloy had the highest corrosion resistance among the uncoated samples. The hydroxyapatite bioceramic coatings also improved the corrosion properties of all samples. However, among all samples, the highest corrosion resistance was obtained in the hydroxyapatite coated AZ91 alloy.

Key words: Hydroxyapatite; AZ Mg alloys; Sol-gel; Corrosion

AZ Serisi Mg Alaşımlarında Hidroksiapatitin Korozyon Davranışı Üzerine Etkisi

Öz: Metalik biyomalzemeler, özellikle ortopedik uygulamalarda yaygın olarak kullanılmaktadır. Mevcut metalik biyomalzemelere alternatif, yüksek spesifik mukavemete, yüksek korozyon direncine ve yüksek biyouyumluluğa sahip yeni alaşımlar geliştirebilmek için pek çok çalışma yapılmaktadır. Mg alaşımları özellikle düşük yoğunluk ve yüksek biyouyumluluğu ile umut vaadeden bir alaşımdır. Ancak özellikle korozyon özelliklerinin geliştirilmesi gerekmektedir. Bu çalışmada biyomalzeme olarak umut vadeden AZ31, AZ61 ve AZ91 alaşımlarının yüzeyleri yüksek biyouyumluluğa sahip hidroksiapatit ile kaplanarak, kaplamaların korozyon direncine etkileri kapsamlı olarak incelenmiştir. Tüm biyoseramik kaplamalarda çatlaksız ve gözenekli yüzey morfolojileri elde edilmiş ve EDS analizleri ile kaplamaların yüzeylerdeki varlığı desteklenmiştir. SBF içerisinde yapılan korozyon testleri sonucunda kaplamasız numuneler arasında en yüksek korozyon dayanımına AZ91 alaşımının sahip olduğu tespit edilmiştir. Hidroksiapatit biyoseramik kaplama, tüm numunelerde de korozyon özelliklerini iyileştirmiştir. Bununla birlikte en yüksek korozyon dayanımı hidroksiapatit kaplı AZ91 alaşımında elde edilmiştir.

Anahtar kelimeler: Hidroksiapatit, AZ Mg Alaşımları, Sol-Gel, Korozyon

1. Introduction

The basic features that biomaterials should have in order to be used safely in orthopedic applications; biocompatibility, corrosion resistance, wear resistance, mechanical compatibility and osteointegration [1,2]. Metallic biomaterials are widely used in the orthopedic and dental applications owing to their advanced biocompatibility and sophisticated mechanical properties. Commonly used traditional metallic implant materials are low-carbon stainless steel, cobalt, and titanium alloys. These alloys have highly improved mechanical properties compared to body tissues (e.g. bone and tooth). However, the fact that the implant has very high strength values compared to the tissue causes load distribution imbalances between the tissue and the implant. In tissue-implant interaction, this biomechanical uncompatibility is called “stress shielding effect” and this is a negative situation that reduces the life of the implant [3,4]. However, the high density values of these alloys cause tissue-implant incompatibility and various complications [5,6]. This causes implant loss and requires a second surgical operation. Therefore, it is very important to develop new biocompatible materials with sufficient strength and low density. Magnesium alloys have high specific strength (strength/density) [3,7-10] and low density values [11,12]. Hence, magnesium alloys are a potential alloy for orthopedic applications due to their low density value, near-bone elastic modulus and biocompatibility [13-17]. However, the biodegradable behavior of magnesium alloys limits the use of these materials. Magnesium has a very low corrosion potential and is more active than most metals

ORCID Number of author: [1] 0000-0001-5005-8516

at 25°C. Therefore, it has a particularly high susceptibility to galvanic corrosion [18]. Implant materials used in in-vivo applications are exposed to body fluids containing various anions (Cl^-, HCO_3^-, HPO_4^{-2}), cations (Na^+, K^+, Ca^{+2}, Mg^{+2}) and dissolved oxygen [19, 20]. Therefore, the human body is a highly corrosive environment for metals used as biomaterials. Chloride, in particular, degrades the semi-passive unstable layer formed on the surface of magnesium as a result of various reactions and causes local degradation. Therefore, it is very difficult to use biodegradable metals (such as Mg alloys) as implant materials in in-vivo applications [21]. Therefore, it is necessary to improve the corrosion properties of these alloys, which have low density and low elastic modulus [22, 23]. In order to prevent or reduce corrosion, it is necessary to prevent the diffusion of corrosive media such as water, oxygen, acid to the surface. For this purpose, metallic surfaces are coated with materials that are stable against corrosive environments. However, bioceramic coatings are made not only to improve corrosion resistance, but also to provide metallic implants with bioactivity and antibacterial properties, and to increase biocompatibility, abrasion and creep resistance [24-27].

Different surface modifications are generally preferred in order to improve the interaction of the metallic implant with the tissue and to increase its corrosion resistance and biocompatibility. The most commonly used materials for surface modifications of metallic implants are hydroxyapatite, bioactive glass and glass ceramics [12,28]. Hydroxyapatite (HA), which is a biodegradable or absorbable biocompatible material, is capable of forming strong chemical bonds with natural bone tissue due to its characteristic properties [29-31]. Due to its bone-like structure, HA allows tissue development of the bone and thus provides significant advantages in terms of osteointegration in orthopedic applications [32]. Besides, it improves biocompatibility and corrosion resistance and helps to prevent ion release as a physical barrier. For this reason, it is generally preferred as the surface coating material of metallic implants [33-35]. Surface modifications of metallic implants can be made using different techniques [36-39]. It is possible to obtain homogeneous solutions at low temperatures with the sol-gel method. For this reason, it is a more advantageous and easier method compared to other methods [40,41].

In order to demonstrate a possible alternative usage of AZ series Mg alloys in low load bearing biomedical applications, corrosion resistances of sol-gel derived Hydroxyapatite based bioceramic dip-coating on AZ31, AZ61 and AZ91 alloys are investigated in this work.

2. Experimental Procedure

2.1. Materials

AZ31, AZ61 and AZ91 Alloys has been used as substrate. AZ series samples were cut in the sizes of 10x20x5 mm. Firstly, the substrates were sand blasted by SiO_2 particles before the coating process in order to improve adhesion of the coating. Sand blasted process with SiO_2 particles (90 µm) at 6 bar pressure was applied onto surfaces. Finally, they were ultrasonically cleaned in distilled water, acetone, and ethanol in order to remove the contaminants and made ready for the coating process.

2.2. Surface Coating

Substrates were coated by sol gel dipcoating technique. The dipping sol fort the coatings were prepared by usingh HA powder with a approximately 10 µm and to ease gelation and sinterability P_2O_5, KH_2PO_4 and $NaCO_3$ inorganic materials as additives were added. Before sol gel process commercial pure hydroxyapatite (HA) and $NaCO_3$ powders were dried in incubator at 80 °C to avoid agglomeration. The prepared sol was ultrasonically homogenized until a homogenous gel was obtained. After the gel was formed, the substrates were dipped into the gel and dip-coated at an immersion rate of 5 mm/s. Coated samples were kept under room conditions and then they were subjected to the pre-drying in the furnace and later subjected to sintering process at 500 °C (3 °C/min) for 120 min in a vacuum environment.

2.3. Corrosion Tests

The corrosion tests were performed by potentiodynamic polarization technique (PDP) in GAMRY PCI14/750 (USA) corrosion test unit in order to examine the effect of the coatings on corrosion resistance of AZ alloys. In corrosion tests, Ringer solution was used as the electrolyte and the temperature of the corrosion cell was fixed to the body temperature (37 °C). All the analyses were performed by using the three electrodes technique. Saturated silver/silver chloride (Ag/AgCl), platinum wire (Pt), and the already prepared corrosion samples were used as reference electrode (RE), counter electrode (CE), and working electrode (WE), respectively. A minimum of 2 tests

were performed for each sample group until the steady state was determined. Open circuit potential measurements (OCP) and potentiodynamic polarization measurements (PDS) were carried out at the scanning rates of 1 mV/s.

2.4. Surface Analyses

Microstructural characterization studies and film thickness of the coated samples were examined by using scanning electron microscopes (SEM, Jeol JSM-6335F) with attachment energy dispersive spectroscopy (EDS). Improving the image quality for before microstructural observations, samples were coated with Au-Pd alloy. However, coating thicknesses were measured using SEM that views taken from the cross section of the samples and mean coating thickness values were then determined.

3. Results and Discussion

In order to improve osseointegration in bioceramic coatings, it is desired that the coating has biocompatible and homogeneous surfaces and low crack content [42]. Fig. 1 shows the SEM views of HA coated AZ alloy substrates, before and after corrosion. SEM analyses showed that a porous surface morphology was obtained at low crack intensity and the corrosion caused formation of dimple in the coatings (Fig. 1).

SEM images of surfaces before corrosion show the presence of locally agglomerated regions in bioceramic coatings. Agglomeration intensity on AZ61/HA sample surfaces increased compared to AZ31/HA group samples. SEM images show that the most agglomerated structure is in AZ91/HA coatings. It is thought that the agglomeration intensity on the surfaces is related to the coating thicknesses. SEM images and coating thickness measurements of the cross-sections of HA coated samples are given in Figure 2. While the average thickness value was measured as 3,25 µm in the AZ31 alloy, this value was measured as 6,68 µm and 7,78 µm in the AZ61 and AZ91 alloys, respectively. These results show that the increase in the agglomeration intensity may be related to the increase in the coating thickness. In similar studies, it is clear that there is a relationship between coating thickness and agglomeration [43].

The damage and pits caused by corrosion on the sample surfaces is clearly seen in the SEM images (Fig. 1). Magnesium and its alloys have very low corrosion resistance in high Cl^- environments [44]. Because unlike the protective passive layer formed in metals such as aluminum or stainless steel, an unstable semi-passive magnesium hydroxide layer is formed in magnesium and its alloys. The formation of metal-hydroxyl-chloride complex compounds with the penetration of Cl^- ions into the hydroxide film causes the formation of pits and an increase in the corrosion rate [45]. Furthermore, Cl^- ions cause pitting corrosion in Magnesium alloys [46]. Although the damages in bioceramic coatings after corrosion is close to each other, it would be more sensible to evaluate the corrosion resistance properties of the samples together with the OCP and PDS analysis results.

EDS analysis results obtained from the surfaces of HA coated AZ alloys are presented in Table 1 and EDS analysis results from cross-sections are presented in Figure 3. Ca, P, O and Mg were detected on all bioceramic coated surfaces. It is thought that the differences in the amount of Mg are affected by the form and distribution of the porosity in the coatings. In addition, differences were determined in the amount of Ca, P and Ca/P ratio. As it is known, the Ca/P ratio in the HA structure is expected to be 1.62 [47]. However, the EDS analysis results show that this ratio was only achieved in the AZ61/HA sample. For this reason, local EDS analyzes were performed on the bioceramic coated sample surfaces and the Ca/P ratio was confirmed in all coatings (Figure 4). The local EDS analysis results given in Figure 4 show that the Ca/P ratio is 1,62 in agglomerated structures and the Mg content is quite low (2,86% wt). The fact that the Mg content in the general surface EDS analysis results given in Table 1 is higher than the local EDS results (Figure 4) is thought to be due to the porous structure of the coating.

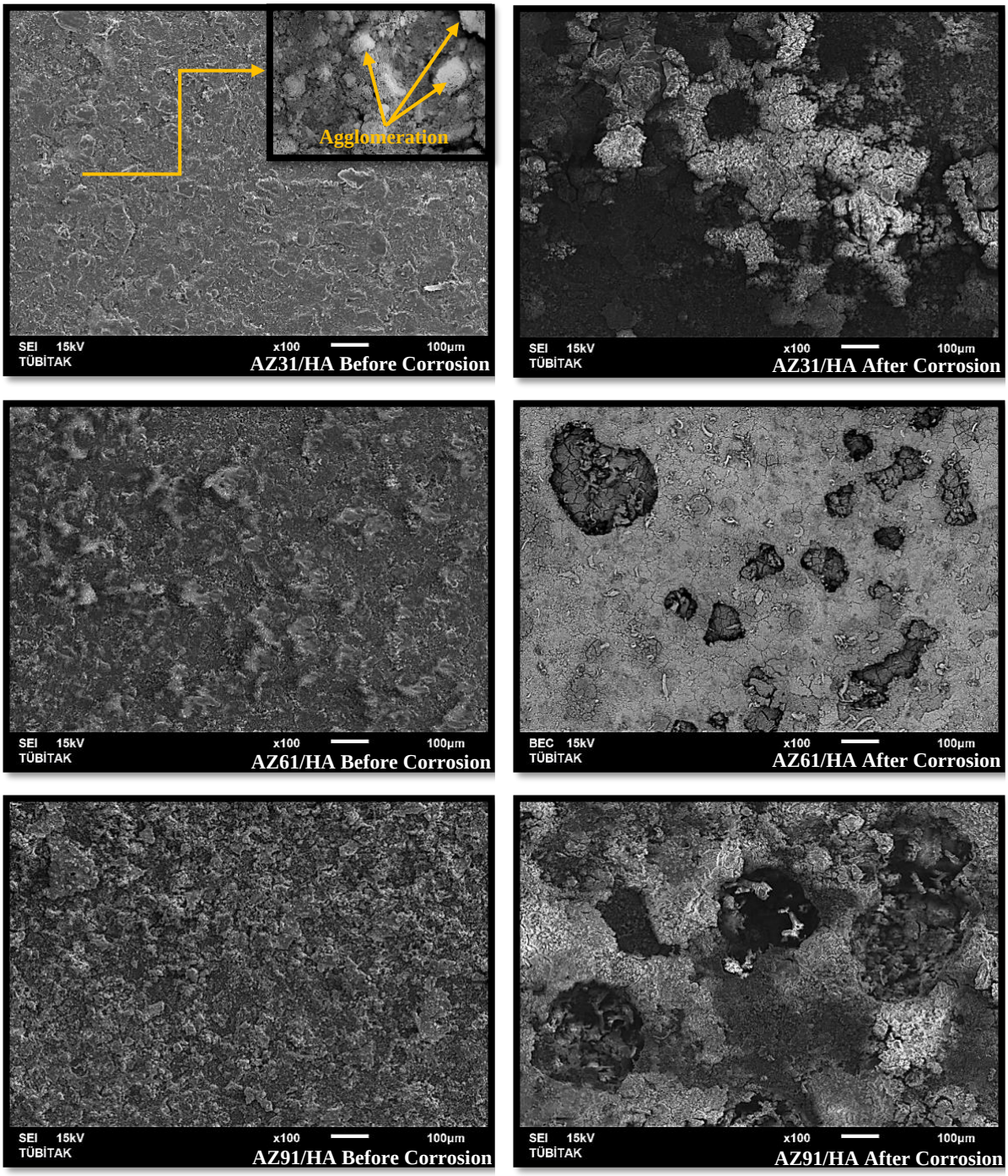

Figure 1. SEM views of coated surfaces before corrosion and after corrosion

Table 1. HA coated AZ Alloy surfaces EDS analysis results.

Sample	Element (wt. %)						Ca/P Rate
	Mg	Al	Zn	Ca	P	O	
AZ31/HA	45,49	-	-	11,80	8,59	34,12	1,3737
AZ61/HA	30,13	-	-	18,92	11,69	39,26	1,6185
AZ91/HA	31,85	-	-	16,06	10,45	42,44	1,5368

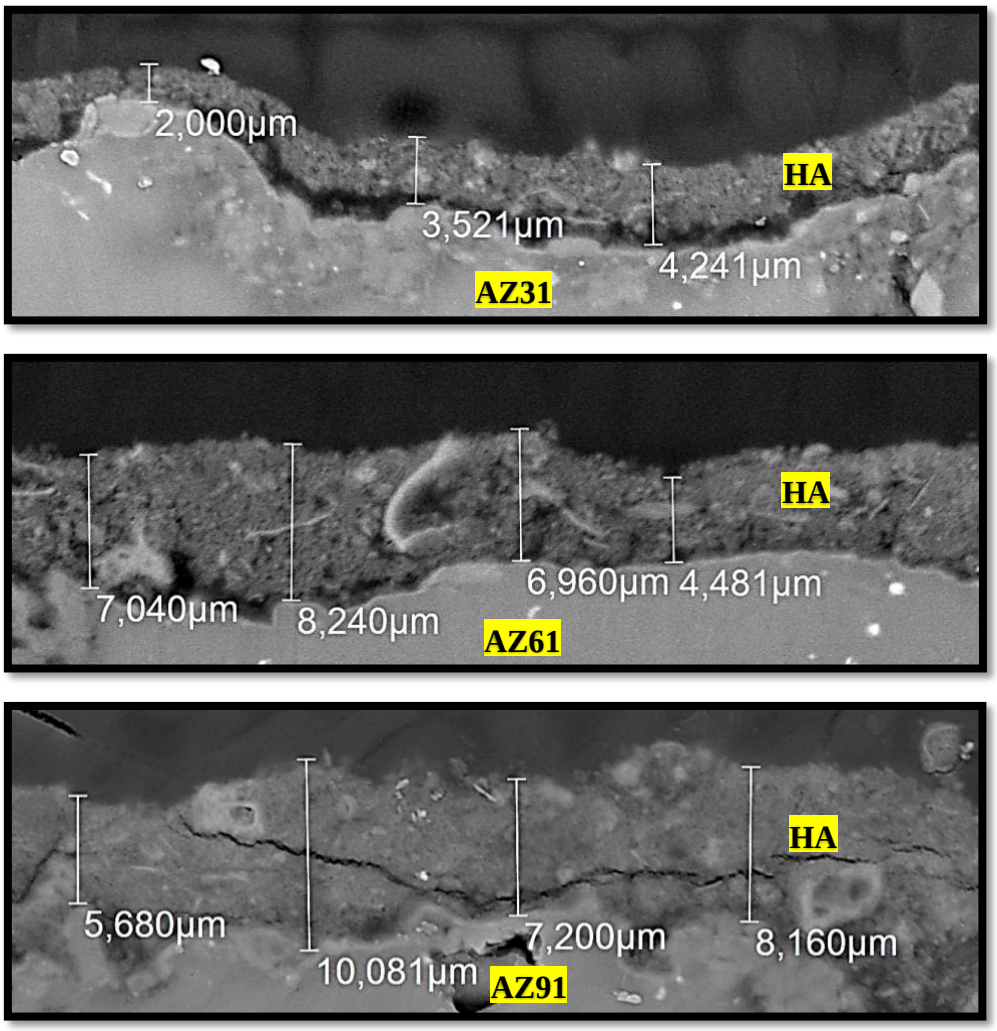

Figure 2. Cross-sectional images and coating thickness measurements of bioceramic coatings

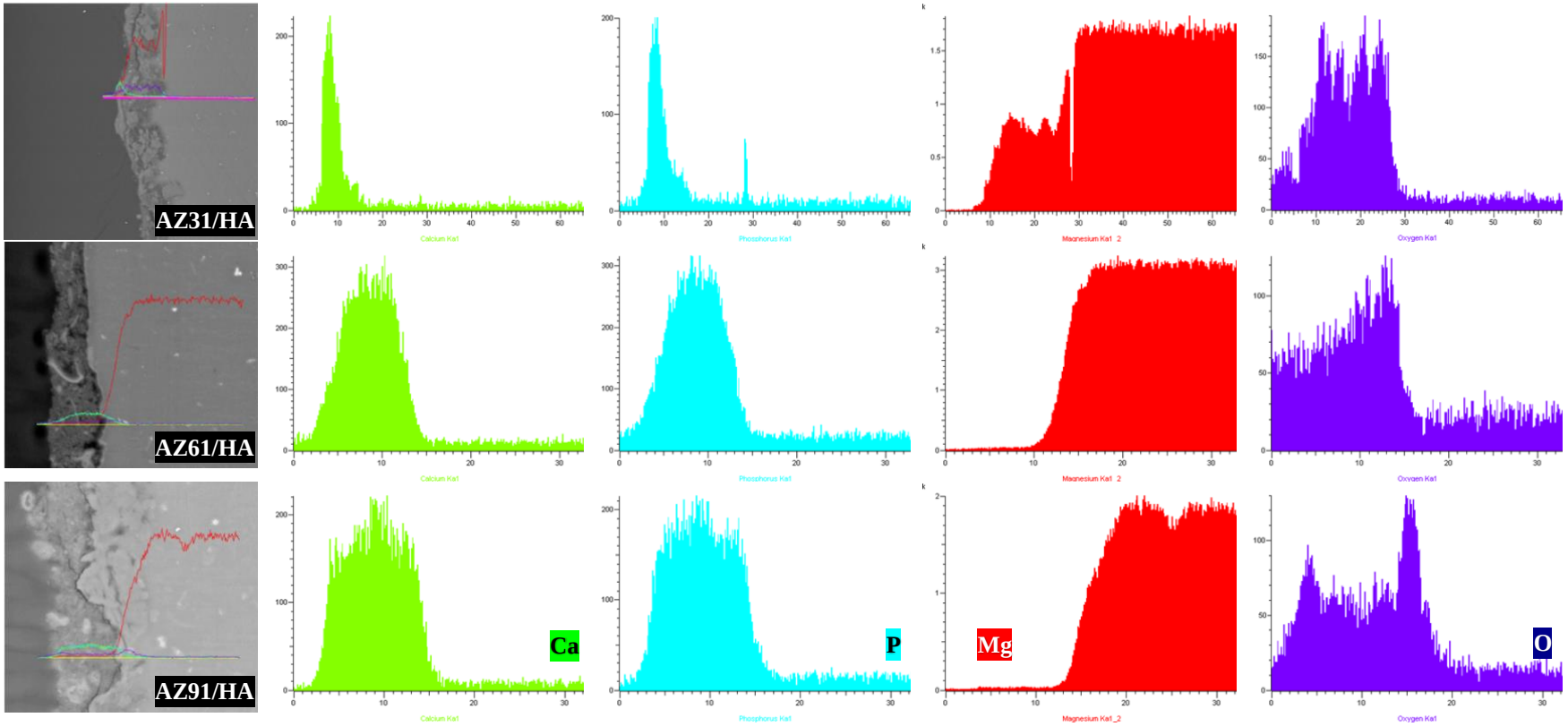

Figure 3. Cross-Sectional EDS analyzes of HA coated AZ series alloys

ORCID Number of author: [1] 0000-0001-5005-8516

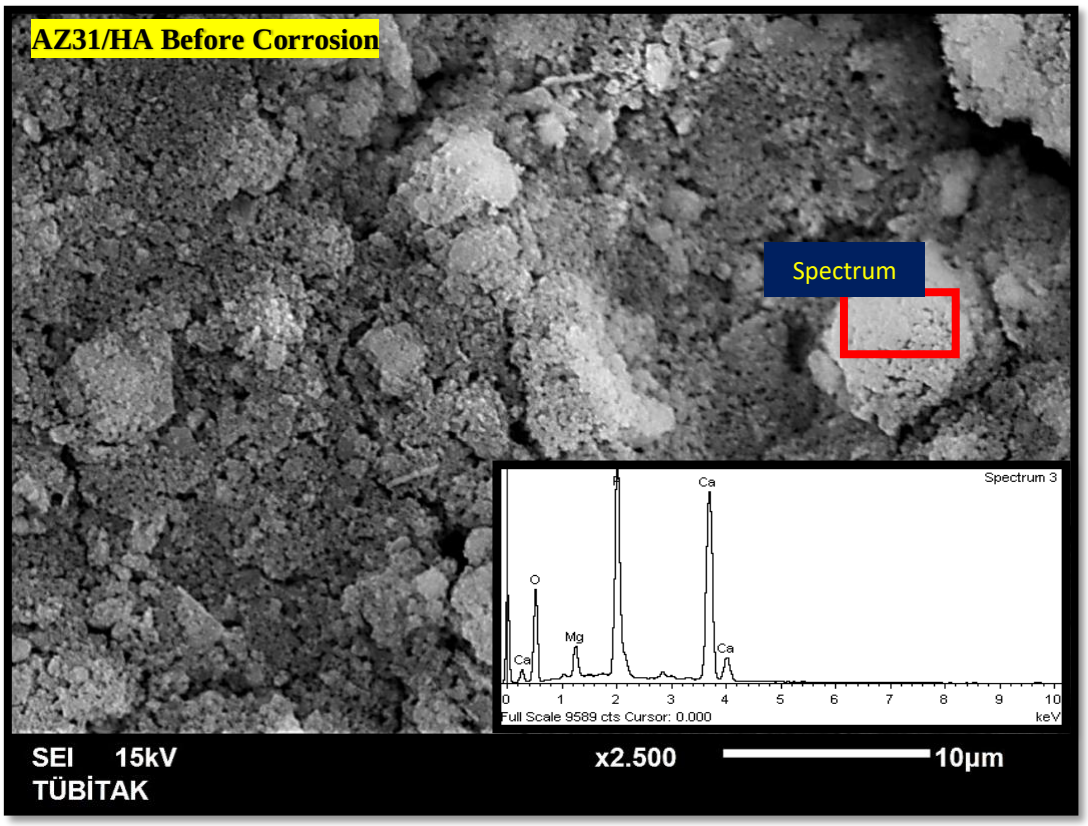

Element (wt. %)						Ca/P Rate
Mg	Al	Zn	Ca	P	O	
2,86	-	-	35,32	21,20	40,62	1,6257

Figure 4. Local EDS analysis results on HA coated AZ31 alloy surface before corrosion

In Figure 5, the EDS analysis results obtained from the inner and outer regions of the pits formed after corrosion on the bioceramic coated surfaces are given. While the Ca-P structure was clearly detected in the outer region of the pit (Spectrum 1), Ca-P could not be detected in the pit region (Spectrum 2). The high rate of Cl^- (16,69 wt. %) detected in the pit region shows that the Cl^- ions in the Ringer solution are highly effective in corrosion. Similar results were obtained in the line EDS analyzes performed on the pits (Fig. 6). While Ca-P dominates the structure throughout the coating, the inside of the pit is almost entirely composed of Mg-Cl-O. These results show that the coating is completely destroyed, especially in the region where the pits are formed, and the corrosion reaches the substrate. It is thought that the porous structure of the coating reduces the corrosion resistance and causes localized corrosion on the bioceramic coated sample surfaces. These pores are regions where the electrolyte remains static. The increase in the concentration of Cl^- ions in these regions causes the formation of localized regions where the solubility of the oxide film and the surface conductivity increase. In other words, these porosities may have acted as preferential corrosion sites.

Areas where passive $Mg(OH)_2$ and MgO layers on magnesium alloys surfaces are destroyed are susceptible to pitting. Cl^- ions penetrate these areas and activate the area [48,49]. However, ions in the body (especially Cl^-) cause the environment to become aggressive in terms of corrosion. Especially cracked and porous surface morphologies are areas where the electrolyte is static and cause local areas of high corrosion sensitivity [50]. The accumulation of Cl^- ions in these regions causes the disruption of the magnesium hydroxide layer and ultimately the degradation of magnesium [21].

ORCID Number of author: [1] 0000-0001-5005-8516

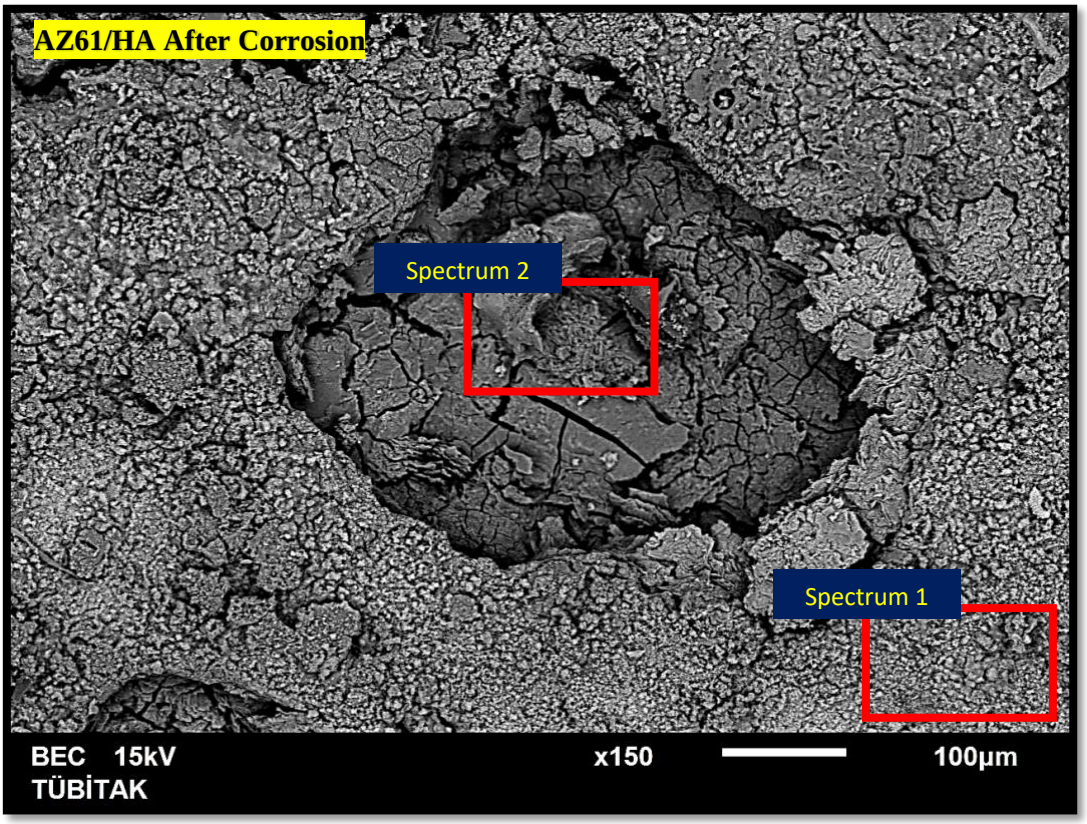

Spectrum	Element (wt. %)				
	Mg	Ca	P	Cl	O
Spectrum 1	20,38	19,22	15,77	-	44,63
Spectrum 2	31,88	-	-	16,69	51,43

Figure 5. Local EDS analysis results on HA coated AZ31 alloy surface after corrosion

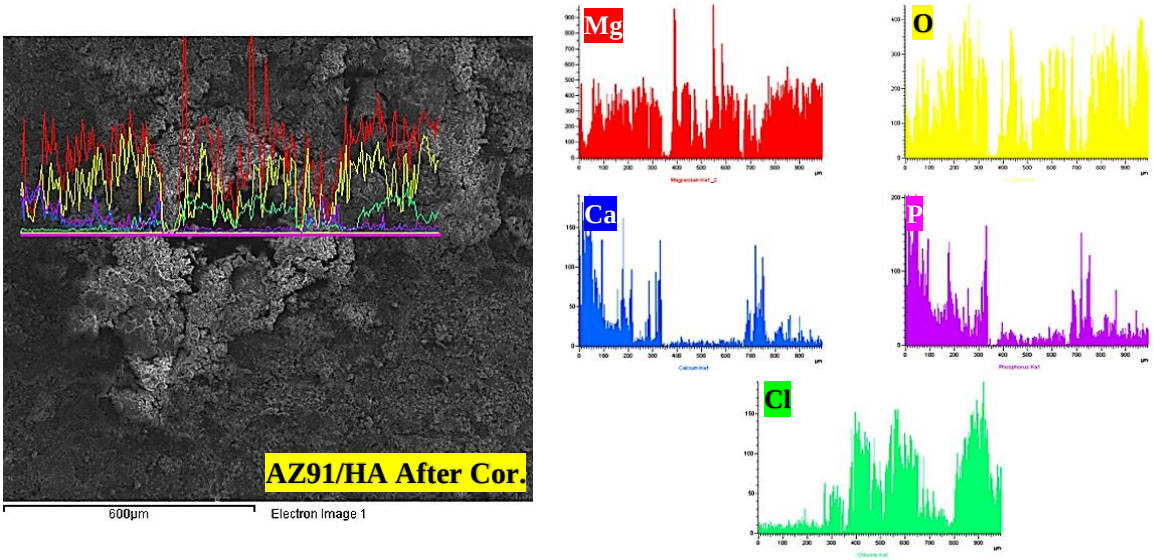

Figure 6. Pitting formation in HA coated AZ91 alloy

OCP analysis results of uncoated and HA coated samples are given in Figure 7. It was observed that E_{OCP} values increased with time in all uncoated and HA coated samples. In addition, it was observed that there was no significant change in E_{OCP} values after an immersion period of approximately 30 minutes in all curves. OCP analysis results of HA coated samples showed that the time to reach stable state was shorter for AZ61/HA sample compared to AZ31/HA and AZ91/HA samples. However, only OCP analyzes are not sufficient to evaluate corrosion properties. Therefore, the corrosion properties were interpreted together with the PDS curves obtained by potentiodynamic analysis.

In Figure 8, the potentiodynamic (PDS) polarization curves of uncoated and AZ alloys coated with HA bioceramic in Ringer solution and at body temperature are presented comparatively. The potentiodynamic polarization method is a very useful method in the determination of the quality and stability of the coating by electrochemical techniques to examine the corrosion that occurs starting from the coated surface. The samples were over-polarized in the anodic direction with the PDS method. The samples were first exposed to free corrosion for a certain period of time. Then, by increasing the potential, corrosion differentiations were determined. Some corrosion parameters (E_{ocp}, E_{corr}, I_{corr}, β_A and β_C, Corrosion Rate) calculated from these curves for different coating groups are given in Table 2.

In the PDS curves, it is observed that the potential increases and the current decreases regularly in the cathodic region for all coatings. However, in all samples, it is observed that the corrosion current density increases significantly in the anodic region. This indicates that the Ringer solution has a significant corrosive effect on the samples and an activation-controlled corrosion mechanism occurs in all coatings. Therefore, it is decisive to compare the I_{corr} values in determining the corrosion behavior. When uncoated AZ alloys are compared with each other, I_{corr} values of AZ31, AZ61 and AZ91 alloys were measured as 3480, 621 and 97,2 nA/cm^2, respectively. These results show that the sample with the highest corrosion resistance on uncoated surfaces is AZ91 alloy. However, it was determined that there was a significant decrease in I_{corr} values in all samples after the alloy surfaces were coated with HA. I_{corr} values for AZ31/HA, AZ61/HA and AZ91/HA alloys were measured as 947, 159 and 32,40 nA/cm^2, respectively. This decrease in I_{corr} values after the surfaces were coated with HA indicates that the corrosion resistance properties of all samples were improved with HA bioceramic coatings. The results show that the I_{corr} value of the AZ31 alloy, which was 3480 nA/cm^2 before coating, decreased to 947 nA/cm^2 after coating, thus a decrease of 72%. Similarly, these decreases were calculated as 74% and 66% for AZ61 and AZ91 alloys, respectively. In addition, while the corrosion rate values of uncoated AZ31, AZ61 and AZ91 alloys were measured as 2940 – 525,3 and 80,89 mpy, respectively, these values were measured as 788,1 – 134,9 and 28,04 mpy, after the HA bioceramic coatings on the sample surfaces. These results show that a significant increase in corrosion resistance (73%, 74% and 65%, respectively) was achieved in all sample groups with HA bioceramic coatings.

Table 2. Corrosion parameters obtained as a result of corrosion tests

Sample	E_{ocp} (mV)	E_{corr} (mV)	I_{corr} (nA/cm2)	βa (mV/dec.)	βc (mV/dec.)	Corrosion Rate (mpy)
AZ31	-1460	-1360	3480	382,1	892,4	2940
AZ61	-1463	-1350	621	69,9	332,2	525,3
AZ91	-1440	-1230	97,2	48,2	243,5	80,89
AZ31/HA	-1462	-1355	947	155,1	311,3	788,1
AZ61/HA	-1506	-1252	159	78,50	277,9	134,4
AZ91/HA	-1476	-1114	32,40	37	236,9	28,04

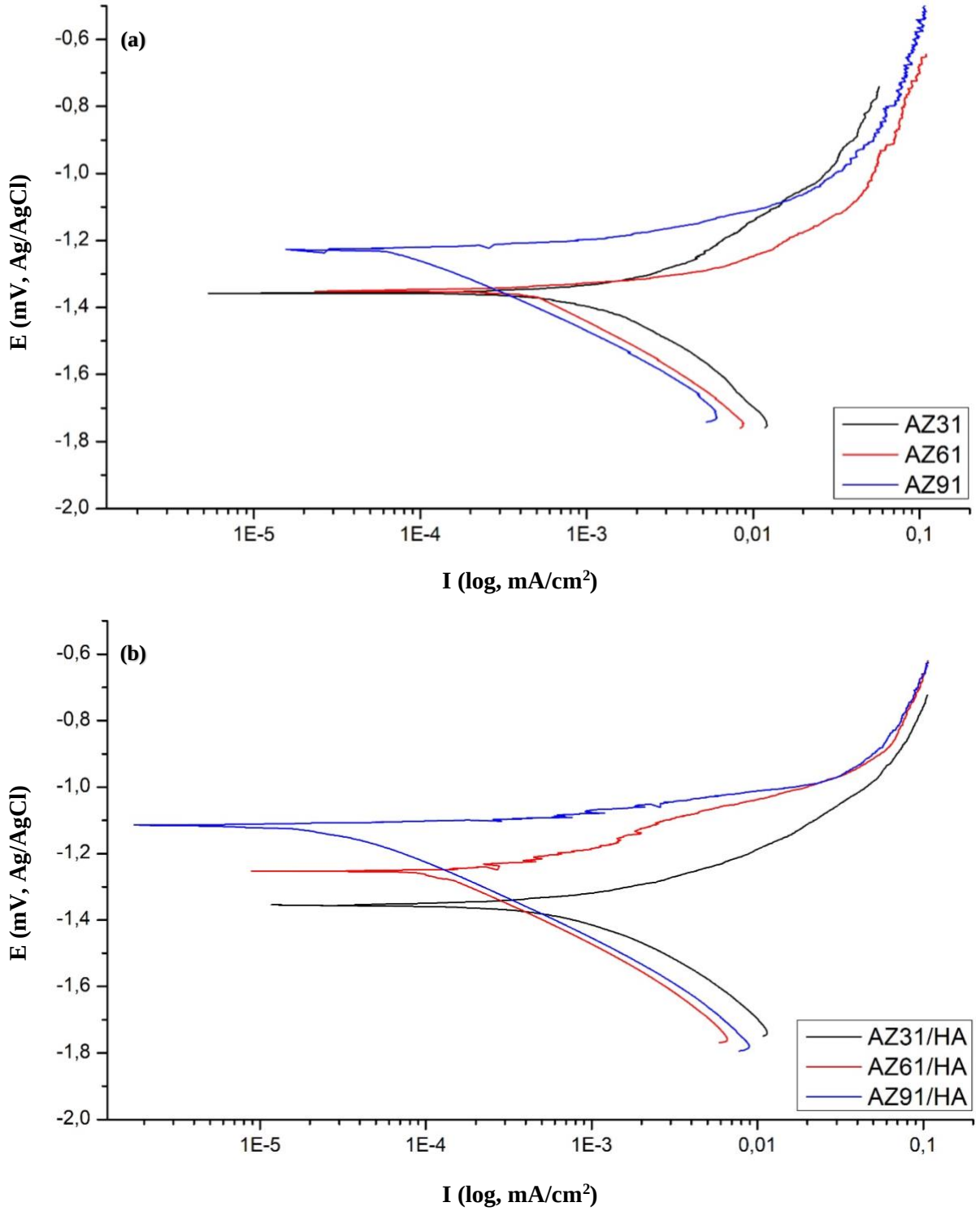

Figure 8. PDS analysis results of uncoated (a) and HA coated (b) samples

As the corrosion potential value increases positively and the current density value decreases, the corrosion rate decreases [51]. In addition, when the potential approaches zero, it means that passivation has started in the surfaces [52]. Compared to the uncoated sample, E_{corr} values were observed to be more noble in all bioceramic coatings. Therefore, the surface reactivity of AZ alloys after coating decreased significantly. The results show that AZ91/HA is the best sample in terms of corrosion resistance among all samples.

In theory, the current flowing through the unit anode surface area gives the corrosion rate [51]. Corrosion rates in uncoated AZ31, AZ61 and AZ91 samples were measured as 2940 – 525,3 and 80,89 mpy, respectively. The corrosion rate decreased in all samples after coating and was measured as 788,1 – 134,4 and 28,04 mpy for AZ31/HA, AZ61/HA and AZ91/HA, respectively. In orthopedic applications, long-term implant materials, at 37 °C solution, 0,5 mm annual degradation rate is desired and this value corresponds to approximately 19,7 mpy [53]. These results, it was determined that the closest result to this desired value was obtained with AZ91/HA (28,04 mpy).

4. Conclusions

The general results obtained as a result of the study are summarized below;

- Crack-free and porous surface morphologies were obtained in all HA bioceramic coatings.
- Coating thickness values of AZ31, AZ61 and AZ91 alloys were measured as 3,25 – 6,68 and 7,78 µm, respectively.
- Agglomerated structures were detected in the coatings and it was determined that the agglomeration intensity increased with the increase of the coating thickness.
- Pit formation was observed in the coatings after corrosion.
- It has been determined that AZ91 alloy exhibits the highest corrosion resistance on uncoated metallic sample surfaces.
- The results show that the Icorr value of the AZ31 alloy, which was 3480 nA/cm^2 before coating, decreased to 947 nA/cm^2 after coating, thus a decrease of 72%. Similarly, these decreases were calculated as 74% and 66% for AZ61 and AZ91 alloys, respectively.
- After HA bioceramic coating, the corrosion rate of AZ31, AZ61 and AZ91 alloys decreased and corrosion resistance increased.
- It was determined that the sample with the highest corrosion resistance and the lowest corrosion rate among all sample groups was the AZ91/HA sample.

References

[1] Hornberger H, Virtanen S, Boccaccini AR. Biomedical coatings on magnesium alloys–a review. Acta Biomater 2012; 8(7): 2442-2455.

[2] Manivasagam G, Dhinasekaran D, Rajamanickam A. Biomedical implants: corrosion and its prevention-a review. Recent Patents on Corrosion Science 2010; 2(1): 40-54.

[3] Jamesh MI, Wu G, Zhao Y, McKenzie DR, Bilek MM, Chu PK. Electrochemical corrosion behavior of biodegradable Mg–Y–RE and Mg–Zn–Zr alloys in Ringer's solution and simulated body fluid. J Corros Sci Eng 2015; 91: 160-184.

[4] Razavi M., Fathi M. H., Meratian M. Microstructure, mechanical properties and bio-corrosion evaluation of biodegradable AZ91-FA nanocomposites for biomedical applications. Mater Sci Eng A 2010; 527(26): 6938-6944.

[5] Hiromoto S, Tomozawa M, Maruyama N. Fatigue property of a bioabsorbable magnesium alloy with a hydroxyapatite coating formed by a chemical solution deposition. J Mech Behav Biomed Mater 2013; 25; 1-10.

[6] Rončević IŠ, Grubač Z, Metikoš-Huković M. Electrodeposition of hydroxyapatite coating on AZ91D alloy for biodegradable implant application. Int J Electrochem Sci 2014; 9: 5907-5923.

[7] Hu J, Wang C, Ren WC, Zhang S, Liu F. Microstructure evolution and corrosion mechanism of dicalcium phosphate dihydrate coating on magnesium alloy in simulated body fluid. Mater Chem Phys 2010; 119(1-2): 294-298.

[8] Wang H, Guan S, Wang Y, Liu H, Wang H, Wang L, Reb C, Zhu S, Chen K. In vivo degradation behavior of Ca-deficient hydroxyapatite coated Mg–Zn–Ca alloy for bone implant application. Colloids Surf B 2011; 88(1): 254-259.

[9] Wang MJ, Chao SC, Yen SK. Electrolytic calcium phosphate/zirconia composite coating on AZ91D magnesium alloy for enhancing corrosion resistance and bioactivity. J Corros Sci Eng 2016; 104: 47-60.

[10] Xiong Y, Lu C, Wang C, Song R. Degradation behavior of n-MAO/EPD bio-ceramic composite coatings on magnesium alloy in simulated body fluid. J Alloys Compd 2015; 625: 258-265.

[11] Fintová S, Kunz L. Fatigue properties of magnesium alloy AZ91 processed by severe plastic deformation. J Mech Behav Biomed Mater 2015; 42: 219-228.

[12] Wang HX, Guan SK, Wang X, Ren CX, Wang LG. In vitro degradation and mechanical integrity of Mg–Zn–Ca alloy coated with Ca-deficient hydroxyapatite by the pulse electrodeposition process. Acta Biomater 2010; 6(5): 1743-1748.

[13] Gopi D, Murugan N, Ramya S, Kavitha L. Electrodeposition of a porous strontium-substituted hydroxyapatite/zinc oxide duplex layer on AZ91 magnesium alloy for orthopedic applications. J Mater Chem B 2014; 2(34): 5531-5540.

[14] Li N, Zheng Y. Novel magnesium alloys developed for biomedical application: a review. J Mater Sci Technol 2013; 29(6): 489-502.
[15] Liu GY, Tang SW, Chuan W, Jin HU, Li DC. Formation characteristic of Ca–P coatings on magnesium alloy surface. Trans Nonferrous Met Soc Chin 2013; 23(8): 2294-2299.
[16] Liu GY, Hu J, Ding ZK, Wang C. Formation mechanism of calcium phosphate coating on micro-arc oxidized magnesium. Mater Chem Phys 2011; 130(3): 1118-24.
[17] Zhang Y, Wei M. Controlling the biodegradation rate of magnesium using sol-gel and apatite coatings. Int J Mod Phys B 2009; 23(06n07):1897-1903.
[18] Gray J, Luan B. Protective coatings on magnesium and its alloys - a critical review. J Alloys Compd 2002; 336(1-2): 88-113.
[19] Ratner BD, Hoffman A.S, Schoen FJ, Lemons JE. Biomaterials science: an introduction to materials in medicine. San Diego, California 2004; 162-4.
[20] Kamachimudali U, Sridhar TM, Raj B. Corrosion of bio implants. Sadhana 2003; 28(3): 601-637.
[21] Gerengi H, Kaya E, Cabrini M. Magnezyumun (% 99.95) Biyobozunur Malzeme Olarak Kullanilma Potansiyeli. İleri Teknoloji Bilimleri Dergisi 2017; 6(2): 1-17.
[22] Agarwal S, Curtin J, Duffy B, Jaiswal S. Biodegradable magnesium alloys for orthopaedic applications: A review on corrosion, biocompatibility and surface modifications. Mater Sci Eng C 2016; 68: 948-963.
[23] Atrens A, Liu M, Abidin NIZ. Corrosion mechanism applicable to biodegradable magnesium implants. Mat Sci Eng B 2011; 176(20): 1609-36.
[24] Arnould C, Denayer J, Planckaert M, Delhalle J, Mekhalif Z. Bilayers coating on titanium surface: the impact on the hydroxyapatite initiation. J Colloid Interface Sci 2010; 341(1): 75-82.
[25] Chang YY, Huang HL, Chen HJ, Lai CH, Wen CY. Antibacterial properties and cytocompatibility of tantalum oxide coatings. Surf Coat Technol 2014; 259: 193-198.
[26] Hiromoto S, Inoue M, Taguchi T, Yamane M, Ohtsu N. In vitro and in vivo biocompatibility and corrosion behaviour of a bioabsorbable magnesium alloy coated with octacalcium phosphate and hydroxyapatite. Acta Biomater 2015; 11: 520-530.
[27] Surmeneva MA, Tyurin AI, Mukhametkaliyev TM, Pirozhkova TS, Shuvarin IA, Syrtanov MS, Surmenev RA. Enhancement of the mechanical properties of AZ31 magnesium alloy via nanostructured hydroxyapatite thin films fabricated via radio-frequency magnetron sputtering. J Mech Behav Biomed Mater 2015; 46: 127-136.
[28] Hiromoto S, Tomozawa M. Hydroxyapatite coating of AZ31 magnesium alloy by a solution treatment and its corrosion behavior in NaCl solution. Surf Coat Technol 2011; 205(19): 4711-19.
[29] Kiahosseini SR, Afshar A, Larijani MM, Yousefpour M. Structural and corrosion characterization of hydroxyapatite/zirconium nitride-coated AZ91 magnesium alloy by ion beam sputtering. Appl Surf Sci Adv 2017; 401: 172-180.
[30] Pang X, Zhitomirsky I. Electrodeposition of hydroxyapatite–silver–chitosan nanocomposite coatings. Surf Coat Technol 2008; 202(16): 3815-21.
[31] Tomozawa M, Hiromoto S, Harada Y. Microstructure of hydroxyapatite-coated magnesium prepared in aqueous solution. Surf Coat Technol 2010; 204(20): 3243-47.
[32] Chen Q, Thouas GA. Metallic implant biomaterials. Mater Sci Eng R 2015;, 87: 1-57.
[33] Bakhsheshi-Rad HR, Hamzah E, Ismail AF, Sharer Z, Abdul-Kadir MR, Daroonparvar M, Saud SN, Medraj, M. Synthesis and corrosion behavior of a hybrid bioceramic-biopolymer coating on biodegradable Mg alloy for orthopaedic implants. J Alloys Compd 2015; 648: 1067-71.
[34] Rajendran A, Barik RC, Natarajan D, Kiran MS, Pattanayak DK. Synthesis, phase stability of hydroxyapatite–silver composite with antimicrobial activity and cytocompatability. Ceram Int 2014; 40(7): 10831-38.
[35] Tan L, Yu X, Wan P, Yang K. Biodegradable Materials for Bone Repairs: A Review. J Mater Sci Technol 2013; 29: 503–513.
[36] Barranco V, Carmona N, Galván JC, Grobelny M, Kwiatkowski L, Villegas MA. Electrochemical study of tailored sol–gel thin films as pre-treatment prior to organic coating for AZ91 magnesium alloy. Prog Org Coat 2010; 68(4): 347-355.
[37] Gu XN, Li N, Zhou WR, Zheng YF, Zhao X, Cai QZ, Ruan L. Corrosion resistance and surface biocompatibility of a microarc oxidation coating on a Mg–Ca alloy. Acta Biomater 2011; 7(4): 1880-1889.
[38] Kannan MB. Electrochemical deposition of calcium phosphates on magnesium and its alloys for improved biodegradation performance: A review. Surf Coat Technol 2016; 301: 36-41.
[39] Liu GY, Hu J, Ding ZK, Wang C. Bioactive calcium phosphate coating formed on micro-arc oxidized magnesium by chemical deposition. App Surf Sci 2011; 257(6): 2051-57.
[40] Ma J, Thompson M, Zhao N, Zhu D. Similarities and differences in coatings for magnesium-based stents and orthopaedic implants. J Orthop Transl 2014; 2(3): 118-130.
[41] Wang D, Bierwagen GP. Sol–gel coatings on metals for corrosion protection. Prog Org Coat 2009; 64(4): 327-338.
[42] Yoshida K, Tanagawa M, Kamada K, Hatada R, Baba K, Inoi T, Atsuta M. Silica coatings formed on noble dental casting alloy by the sol-gel dipping process. J Biomed Mater 1999; 46(2): 221-227.

[43] Bakhsheshi-Rad HR, Hamzah E, Shuang CP, Berto F. Preparation of poly (ε-caprolactone)-hydroxyapatite composite coating for improvement of corrosion performance of biodegradable magnesium. Mater Des Process Commun 2020; 2(4): 170
[44] Gozuacik NK, Altay M, Baydogan M. Micro Arc Oxidation of AZ91 Magnesium Alloy–Effect of Organic Compounds in the Electrolyte. In Defect and Diffusion Forum Trans Tech Pub Ltd. 2014; 353: 217-222.
[45] Wang L, Zhang BP, Shinohara T. Corrosion behavior of AZ91 magnesium alloy in dilute NaCl solutions. Mater Des 2010; 31(2): 857-863.
[46] Perez N. Electrochemistry and corrosion science. Boston, MA: Springer Us. 2004.
[47] Wang H, Lee JK, Moursi A, Lannutti JJ. Ca/P ratio effects on the degradation of hydroxyapatite in vitro. J Biomed Mater Res Part A 2003; 67(2): 599-608.
[48] Pe PAS. Fundamentals of corrosion: Mechanisms, causes, and preventative methods. CRC Press, 2009.
[49] Song GL. Corrosion of magnesium alloys. Elsevier, 2011.
[50] Tahmasebifar A, Kayhan SM, Evis Z, Tezcaner A, Çinici H, Koc M. Mechanical, electrochemical and biocompatibility evaluation of AZ91D magnesium alloy as a biomaterial. J Alloys Compd 2016; 687: 906-919.
[51] Callister WD, Rethwisch DG. Materialwissenschaften und Werkstofftechnik: Eine Einführung. John Wiley & Sons, 2012.
[52] El Abedin SZ, Welz-Biermann U, Endres F. A study on the electrodeposition of tantalum on NiTi alloy in an ionic liquid and corrosion behaviour of the coated alloy. Electrochem Commun 2005; 7(9): 941-946.
[53] Erinc M, Sillekens WH, Mannens RGTM, Werkhoven RJ. Applicability of existing magnesium alloys as biomedical implant materials. TNO Industrie en Techniek, 2009.